Journal of Sustainability for Energy
https://www.acadlore.com/journals/JSE

A Coupled Dynamic Model of HVAC Energy Demand, Cabin Thermal Conditions, and Air Quality in Passenger Cars

Andrea Colantoni [1,2*], Antonio Marcantuono[3], Roberto Romano[3]

[1] Interdepartmental Center for Research and Diffusion of Renewable Energy (CIRDER), Tuscia University, 01100 Viterbo, Italy
[2] Department of Agricultural and Forestry Sciences (UNITUS-DAFNE), Tuscia University, 01100 Viterbo, Italy
[3] Area Ricerca e Sviluppo, DR Automobiles S.r.l., 86070 Isernia, Italy

* Correspondence: Andrea Colantoni (Email: colantoni@unitus.it)

Received: 08-12-2026 **Revised:** 10-22-2026 **Accepted:** 11-03-2026

Citation: A. Colantoni, A. Marcantuono, and R. Romano, "A coupled dynamic model of HVAC energy demand, cabin thermal conditions, and air quality in passenger cars," *J. Sustain. Energy*, vol. 5, no. 4, pp. 322–337, 2026. https://doi.org/10.56578/jse050404.

© 2026 by the author(s). Published by Acadlore Publishing Services Limited, Hong Kong. This article is available for free download and can be reused and cited, provided that the original published version is credited, under the CC BY 4.0 license.

Abstract: Ventilation strategies influence the energy demand of passenger-car heating, ventilation, and air-conditioning (HVAC) systems by changing outdoor-air loads, occupant-generated carbon dioxide (CO_2) accumulation, and particle ingress. Assessing these competing effects requires consistent treatment of cabin heat transfer, moisture, airflow, and filtration. This study investigates the energy–air-quality trade-offs associated with alternative cabin ventilation strategies using a reduced-order dynamic model. Transient heat and moisture balances were coupled with occupant-generated CO_2, fine particulate matter ($PM_{2.5}$) transport and filtration, and HVAC electrical demand. Fresh-air operation, high recirculation, and a rule-based switching strategy were compared in an illustrative 30-min summer simulation with four occupants. Under high recirculation, the predicted end-of-period CO_2 concentration reached approximately 7,059 ppm, compared with 1,030 ppm under fresh-air operation. The corresponding $PM_{2.5}$ concentrations were approximately 6.7 and 35.0 μg/m^3, while cumulative HVAC electricity use was 0.332 and 0.379 kWh, respectively. High recirculation therefore reduced simulated electricity use by 12.4% but allowed substantially greater CO_2 accumulation. The rule-based strategy consumed 0.378 kWh and produced final CO_2 and $PM_{2.5}$ concentrations close to those of continuous fresh-air operation. These model-based results indicate that cabin energy savings must be assessed alongside ventilation and pollutant exposure requirements. The framework provides a common basis for comparing HVAC electricity demand and cabin environmental conditions under prescribed ventilation configurations.

Keywords: Vehicle heating, ventilation, and air-conditioning; Energy efficiency; Cabin thermal environment; Indoor air quality; Air recirculation; Reduced-order modeling

1 Introduction

1.1 Cabin Ventilation and Vehicle Energy Demand

Passenger-car heating, ventilation, and air-conditioning (HVAC) systems consume energy to maintain cabin environmental conditions. In battery-electric vehicles, HVAC operation draws on the same stored electrical energy as propulsion, making cabin conditioning an integral part of vehicle energy management. Lee et al. [1] examined passenger electric-vehicle energy consumption under real-world driving conditions and demonstrated the importance of ambient temperature. Zhu et al. [2] reviewed the integration of cabin conditioning, battery cooling, and powertrain thermal management, while Geleta et al. [3] surveyed control strategies for reducing cabin-conditioning energy use while maintaining thermal comfort. These studies connect cabin environmental requirements with vehicle electrical demand.

Ventilation directly affects this relationship. Outdoor air dilutes occupant-generated carbon dioxide (CO_2), but it can also introduce fine particulate matter ($PM_{2.5}$) and increase sensible and latent conditioning loads. Recirculation permits repeated filtration and can reduce outdoor-air conditioning demand while limiting CO_2 removal. Wei et al. [4] examined the effects of recirculation on cabin air quality and energy use across different climates and outdoor particle concentrations. Mohan and Varghese [5] investigated the simultaneous control of CO_2 and $PM_{2.5}$,

addressing their opposing responses to ventilation. Russi et al. [6] combined cabin environmental measurements with HVAC electricity measurements during heating and cooling, and Lesage et al. [7] evaluated air quality and energy consumption through system simulation. Together, these studies show that ventilation strategies require a joint assessment of cabin conditions and electrical demand.

1.2 Cabin Environmental Modeling and Ventilation Control

The representation of cabin thermal conditions depends on the intended engineering application. Zhao et al. [8] reviewed vehicle-cabin thermal models and discussed the relationship between model complexity, boundary conditions, and predictive accuracy. Torregrosa-Jaime et al. [9] developed a dynamic two-zone lumped thermal model and validated it under variable ambient conditions. Their work demonstrates how conservation-based models can describe transient cabin loads while retaining explicit representations of air renewal and solar radiation.

Predicting cabin thermal states and assessing occupant comfort involve different quantities. Chen et al. [10] reviewed thermal-comfort models for nonuniform and transient cabin environments. A subsequent comparative evaluation examined model accuracy, generalizability, and measurement feasibility [11]. ISO 14505-2:2026 specifies an equivalent-temperature approach for evaluating thermal conditions in vehicles [12]. These approaches distinguish mean cabin-air temperature from the thermal conditions experienced by individual occupants. The present study uses mean air temperature and humidity ratio to describe the bulk thermal and moisture states and to calculate conditioning loads.

Pollutant transport requires separate descriptions of internally generated CO_2 and outdoor particles because they respond differently to airflow. Wei et al. [13] developed a size-resolved particle and CO_2 model incorporating recirculation, infiltration, filtration, and deposition. Chang et al. [14] used computational fluid dynamics to investigate ventilation strategies for balancing CO_2 and suspended particle concentrations under different occupancies. These studies show why outdoor-air exchange alone cannot characterize cabin air quality: increasing outdoor airflow can dilute CO_2 while increasing particle ingress.

Filtration further modifies this response. Wang et al. [15] investigated vehicle cabin-filter efficiency, pressure drop, and service life. Renck and Jung [16] examined cabin filters and portable air purifiers, including the dependence of particle-removal performance on HVAC fan settings. Their findings support treating airflow and filtration as separate model inputs. Interpreting cabin air-quality predictions also requires attention to the measurements used for comparison and the meaning of the selected concentration thresholds. Silva et al. [17] reviewed the accuracy, applications, and limitations of low-cost indoor air-quality sensors. Persily [18] clarified that 1,000 ppm CO_2 is not a universal indoor-air-quality limit. Accordingly, the CO_2 thresholds used here specify a ventilation-control policy rather than a general health criterion.

These concentration thresholds connect cabin air-quality assessment with ventilation control, where outdoor-air supply and recirculation are adjusted alongside thermal requirements. Ramesh Babu et al. [19] investigated adaptive recirculation during electric-truck heating using coupled computational fluid dynamics and thermoregulation modeling, with humidity and CO_2 informing the recirculation strategy. Lesage et al. [20] examined CO_2-responsive ventilation in an electric passenger vehicle and related its operation to thermal conditions and energy use. At the integrated thermal-system level, Wang et al. [21] developed model predictive control for cabin and battery temperature management. These studies demonstrate how environmental requirements can guide the selection of energy-efficient operating inputs.

The electrical comparison must account for air circulation as well as heating or cooling. Zhang et al. [22] investigated low-temperature HVAC energy consumption while considering blower efficiency. When ventilation policies use different supply flows or fan settings, their energy difference reflects the complete operating configuration. Reporting airflow, conditioning demand, and fan power separately makes the source of that difference traceable.

Comparing the resulting energy and environmental trajectories requires both consistent physical accounting and checks on the numerical solution. Oberkampf and Roy [23] distinguished numerical verification from physical validation in scientific computing. Ordinary-differential-equation methods [24] and software implementations such as SciPy's integration routines [25] provide tools for solving transient balances. Analytical limiting cases, step-size comparisons, and integrated conservation residuals provide complementary checks on the computed solutions.

Uncertainty propagation and parameter sensitivity provide complementary forms of model assessment. The Joint Committee for Guides in Metrology guides address uncertainty expression and propagation [26, 27], while Morris screening and global sensitivity methods characterize parameter influence over a sampled input domain [28, 29]. The present study uses local finite differences to examine responses around the prescribed summer baseline.

1.3 Research Gap and Contribution

The preceding studies establish the importance of jointly assessing cabin conditions and HVAC energy use. For comparisons across ventilation policies, the remaining methodological task is to keep the airflow pathways, source terms, and electrical accounting consistent and explicit. Controlled outdoor-air supply, infiltration, and recirculation

perform different physical functions. Outdoor air and infiltration exchange heat, moisture, and contaminants with the surroundings, whereas recirculation returns cabin air through the HVAC system and enables repeated filtration. A compact formulation that preserves these distinctions allows differences in cabin conditions and electricity use to be traced to the prescribed operating inputs.

This study develops a reduced-order dynamic model coupling cabin temperature, humidity ratio, CO_2 concentration, and $PM_{2.5}$ concentration with HVAC electrical demand. The formulation integrates occupant sources, heat transfer, outdoor-air exchange, recirculation filtration, and conditioning loads within four state balances and a common electrical-demand calculation. Its methodological contribution is a transparent comparison framework in which changes in cabin conditions and energy use can be traced to the same physical inputs and operating policies.

The model is applied to a prescribed 30-min summer scenario with four occupants. Continuous fresh-air operation, high recirculation, and a CO_2-based switching policy are compared using transient cabin conditions and cumulative electricity consumption. Conditioning and fan-power contributions are reported separately, and switching behavior is interpreted in relation to the CO_2 equilibrium associated with each ventilation mode. The resulting analysis provides a basis for evaluating vehicle HVAC energy efficiency alongside cabin environmental requirements under explicitly defined operating conditions.

2 Engineering Model and Assumptions

2.1 System Boundary and Assumptions

The passenger compartment is represented as a single, well-mixed control volume coupled to the HVAC system and the outdoor environment. Four state variables describe its transient response: mean air temperature, humidity ratio, CO_2 concentration, and $PM_{2.5}$ concentration. HVAC electrical demand is calculated from the conditioning load and air-circulation power. This representation connects cabin environmental conditions to energy use through explicit heat and mass balances, following conservation-based approaches to cabin thermal response and pollutant transport [9, 13].

The model boundary includes heat transfer through the vehicle envelope, solar gains, occupant heat and moisture release, occupant-generated CO_2, outdoor-air exchange, and particle filtration and deposition. The effective cabin volume is denoted by V, while C_{th} represents the combined thermal capacitance assigned to the cabin air and the interior materials participating in the modeled transient. Envelope heat transfer is described by the overall conductance UA. These quantities are effective model parameters; the numerical values used in the summer demonstration are specified in Section 4.

The HVAC supply consists of controlled outdoor air and recirculated cabin air. For a total supply flow Q_{sup} and recirculation fraction r,

$$Q_{\text{oa}} = (1-r)Q_{\text{sup}}\,, Q_{\text{r}} = rQ_{\text{sup}}\,, 0 \le r \le 1$$

where, r applies only to the controlled HVAC supply. Uncontrolled infiltration is represented separately by Q_{inf}, giving the total outdoor-air exchange $Q_{\text{f}} = Q_{\text{oa}} + Q_{\text{inf}}$. At approximately constant cabin pressure and volume, this inflow is balanced by an equal exhaust or exfiltration flow. Recirculation remains internal to the cabin–HVAC system: it enables repeated particle filtration but does not directly dilute cabin CO_2. Outdoor-air exchange, by contrast, transports heat, moisture, and pollutants between the cabin and its surroundings [4, 13].

Figure 1 presents the cabin boundary and HVAC airflow arrangement. Outdoor air and return air enter the mixing section, pass through the filtration and conditioning components, and are supplied to the cabin. Occupant emissions, solar gains, and envelope heat transfer act on the cabin control volume. Particle entry through uncontrolled infiltration is treated separately from filtered outdoor-air supply.

Filtration is represented by effective single-pass removal efficiencies for the outdoor-air and recirculation paths, denoted by η_{f} and η_{r}, respectively. These coefficients account for the particle-removal performance relevant to the modeled $PM_{2.5}$ concentration. For a shared filter exposed to comparable particle distributions and operating conditions, the two efficiencies can be assigned the same value. Separate coefficients allow different filtration arrangements to be represented. Filter performance depends on airflow, particle size, and loading [13, 15, 16]. The present formulation represents these effects through effective removal efficiencies prescribed for each operating condition.

Table 1 summarizes the model parameters, prescribed inputs, and their characterization basis. The values adopted for the illustrative summer scenario are specified in Section 4.

The model assumes well-mixed cabin air, with uniform mean temperature, humidity ratio, and pollutant concentrations. Air properties and effective envelope parameters remain constant within each simulation, and the windows are closed. Supply jets, local radiation asymmetry, breathing-zone gradients, and volatile organic compounds are outside the state description. The thermal states characterize bulk cabin conditions; local occupant-comfort assessment requires additional information on airflow, surface temperatures, and occupant exposure [9–12, 19].

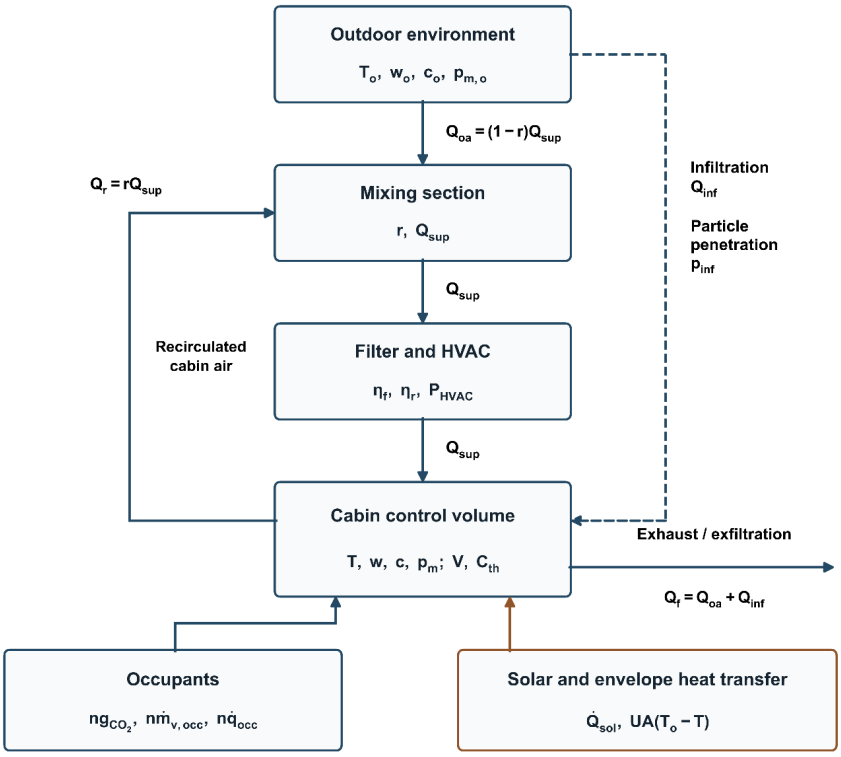


Figure 1. Cabin control volume and HVAC airflow paths

Note: T_o = outdoor temperature; w_o = outdoor humidity ratio; c_o = outdoor CO_2 concentrations; $p_{m,o}$ = outdoor $PM_{2.5}$ concentrations; Q_{oa} = flow rate of controlled outdoor air supplied by the HVAC system; r = recirculation fraction; Q_{sup} = supply airflow; Q_{inf} = uncontrolled outdoor-air exchange; p_{inf} = infiltration penetration factor; Q_r = flow rate of recirculated cabin air within the HVAC supply; η_f or η_r = filter efficiencies; P_{HVAC} = total electrical power demand of the HVAC system; T = cabin temperature; w = cabin humidity ratio; c = cabin CO_2 concentrations; P_m = cabin $PM_{2.5}$ concentrations; C_{th} = thermal capacitance; Q_f = total outdoor-air exchange rate; n = occupancy; g_{CO_2} = CO_2 generation; $\dot{m}_{v,occ}$ = occupant moisture generation; $\dot{q}_{occ}$ = per-person sensible heat; $\dot{Q}_{sol}$ = solar heat gain rate; UA = envelope conductance; HVAC = heating, ventilation, and air-conditioning; CO_2 = carbon dioxide; $PM_{2.5}$ = fine particulate matter.

Table 1. Model parameters, prescribed inputs, and characterization basis

Parameter or Input	Physical Meaning	Characterization Basis
V, C_{th}, UA	Effective cabin volume, thermal capacitance, and envelope conductance	Vehicle geometry, thermal characterization, or stated engineering assumptions
Q_{sup}, r, Q_{inf}	Supply airflow, recirculation fraction, and uncontrolled outdoor-air exchange	HVAC airflow data, leakage characterization, or prescribed scenario values
η_f, η_r, p_{inf}, k_d	Filter efficiencies, infiltration penetration factor, and particle deposition rate	Component data, relevant literature, or stated assumptions
T_o, w_o, I_{sol}	Outdoor temperature, humidity ratio, and solar irradiance	Environmental records or prescribed boundary conditions
c_o, $p_{m,o}$	Outdoor CO_2 and $PM_{2.5}$ concentrations	Monitoring data or prescribed concentrations
n, $\dot{q}_{occ}$, $\dot{m}_{v,occ}$, g_{CO_2}	Occupancy and per-person sensible heat, moisture, and CO_2 generation	Occupant activity assumptions or documented source rates
COP_h, COP_c, P_{fan}, P_{aux}	Heating and cooling performance, fan power, and other auxiliary power	Equipment data or stated electrical-demand assumptions

Note: HVAC = heating, ventilation, and air-conditioning; CO_2 = carbon dioxide; $PM_{2.5}$ = fine particulate matter.

Temperature is expressed in kelvin in the governing equations and reported in degrees Celsius. Volumetric flow rates are converted to $m^3 \cdot s^{-1}$ for calculation, thermal and electrical power are expressed in watts, and cumulative electrical energy is reported in kilowatt-hours. Humidity ratio is expressed in kilograms of water vapour per kilogram of dry air. CO_2 is calculated as a dimensionless volume fraction and reported in ppm, while $PM_{2.5}$ mass concentration is expressed in $\mu g/m^3$.

2.2 Coupled Conservation Balances and Heating, Ventilation, and Air-Conditioning Demand

The thermal balance combines HVAC sensible conditioning, envelope heat transfer, outdoor-air exchange, solar gain, and occupant sensible heat:

$$C_{\mathrm{th}}\frac{\mathrm{d}T}{\mathrm{d}t} = \dot{Q}_{\mathrm{HVAC,\,s}} + UA\,(T_{\mathrm{o}} - T) + \rho c_p Q_{\mathrm{f}}\,(T_{\mathrm{o}} - T) + \dot{Q}_{\mathrm{sol}} + n\dot{q}_{\mathrm{occ}} \tag{1}$$

where, T and T_{o} are cabin and outdoor temperatures, ρ is air density, and c_p is its specific heat capacity. The sensible conditioning rate $\dot{Q}_{\mathrm{HVAC,s}}$ is positive for heating and negative for cooling. It represents the thermal energy added or removed by HVAC conditioning, with outdoor-air exchange accounted for separately by the third term. Accordingly, it excludes the ventilation heat-transfer term already included in Eq. (1).

The effective solar load is:

$$\dot{Q}_{\mathrm{sol}} = \alpha_{\mathrm{sol}} A_{\mathrm{sol}} I_{\mathrm{sol}}$$

where, A_{sol} is an effective solar-exposure area and α_{sol} combines the transmission and absorption effects represented by the lumped model. A prescribed solar heat-gain value can equivalently be applied directly. The occupant term uses the sensible heat-release rate per person, $\dot{q}_{\mathrm{occ}}$, so that moisture-related energy is not included twice.

Moisture conservation is formulated using cabin and outdoor humidity ratios, w and w_{o}:

$$m_{\mathrm{da}}\frac{\mathrm{d}w}{\mathrm{d}t} = \dot{m}_{\mathrm{da,f}}\,(w_{\mathrm{o}} - w) + n\dot{m}_{\mathrm{v,occ}} + \dot{m}_{\mathrm{v,HVAC}} - \dot{m}_{\mathrm{v,cond}}, \dot{m}_{\mathrm{da,f}} \simeq \rho_{\mathrm{da}} Q_{\mathrm{f}}$$

The approximately constant dry-air mass is m_{da}, and ρ_{da} is the corresponding dry-air density. Occupant moisture generation is $\dot{m}_{\mathrm{v,occ}}$. The signed HVAC moisture-transfer rate $\dot{m}_{\mathrm{v,HVAC}}$ is negative during coil dehumidification and positive during humidification. The nonnegative term $\dot{m}_{\mathrm{v,cond}}$ represents condensation on interior surfaces. These terms describe separate moisture-removal paths; water removed at the cooling coil is included only in $\dot{m}_{\mathrm{v,HVAC}}$.

Relative humidity is obtained from T, w, and cabin pressure p. The water-vapour partial pressure is:

$$p_{\mathrm{v}} = \frac{pw}{0.622 + w}$$

and relative humidity is calculated as $p_{\mathrm{v}}/p_{\mathrm{sat}}\,(T)$, where p_{sat} is the saturation vapour pressure. A windscreen-condensation assessment additionally requires the interior glass temperature T_{g}. The condition $T_{\mathrm{g}} < T_{\mathrm{dp}}$, with T_{dp} denoting the cabin-air dew-point temperature, identifies the thermodynamic potential for condensation. Glass temperature is an additional prescribed quantity or submodel output; it is not one of the four cabin states.

Figure 2 summarizes how ventilation, occupant sources, conditioning, and filtration connect the thermal and environmental balances.

For CO_2, let c and c_{o} denote cabin and outdoor volume fractions. The balance is:

$$V\frac{\mathrm{d}c}{\mathrm{d}t} = n g_{\mathrm{CO_2}} + Q_{\mathrm{f}}\,(c_{\mathrm{o}} - c) \tag{2}$$

where, $g_{\mathrm{CO_2}}$ is the equivalent volumetric CO_2 generation rate per person, expressed at the reference conditions used for the airflow calculation. Multiplication of c by 10^6 gives the reported concentration in ppm. Recirculated flow does not appear as a dilution term because its CO_2 concentration is that of the returning cabin air. Eq. (2) therefore links occupant-generated accumulation directly to effective outdoor-air exchange, consistent with the distinct roles of recirculation and outdoor-air exchange [4, 5, 13].

The $PM_{2.5}$ mass balance distinguishes filtered outdoor-air entry from particle penetration through infiltration:

$$\begin{aligned} V\frac{\mathrm{d}p_{\mathrm{m}}}{\mathrm{d}t} = {} & (1 - \eta_{\mathrm{f}})\,Q_{\mathrm{oa}} p_{\mathrm{m,o}} + p_{\mathrm{inf}} Q_{\mathrm{inf}} p_{\mathrm{m,o}} \\ & - (Q_{\mathrm{oa}} + Q_{\mathrm{inf}})\,p_{\mathrm{m}} - \eta_{\mathrm{r}} Q_{\mathrm{r}} p_{\mathrm{m}} - V k_{\mathrm{d}} p_{\mathrm{m}} + S_{\mathrm{m}} \end{aligned} \tag{3}$$

where, p_{m} and $p_{\mathrm{m,o}}$ are the cabin and outdoor $PM_{2.5}$ mass concentrations. The first two terms represent particle entry through filtered outdoor-air supply and uncontrolled infiltration, respectively. The infiltration penetration factor p_{inf} is the fraction of outdoor particle concentration transmitted through the leakage path. The subsequent terms describe particle removal by exhaust or exfiltration, recirculation filtration, and deposition, followed by the internal source S_{m}. The deposition coefficient k_{d} has units of s^{-1}, and S_{m} is expressed in $\mu\mathrm{g}{\cdot}\mathrm{s}^{-1}$. This separation preserves the different entry and removal mechanisms associated with each airflow path [13].

HVAC electrical demand combines sensible conditioning, latent cooling, air circulation, and auxiliary loads:

$$P_{\mathrm{HVAC}} = \frac{\max\left(\dot{Q}_{\mathrm{HVAC},s}, 0\right)}{\mathrm{COP_h}} + \frac{\max\left(-\dot{Q}_{\mathrm{HVAC},s}, 0\right) + \dot{Q}_{\mathrm{lat}}}{\mathrm{COP_c}} + \frac{Q_{\mathrm{sup}}\,\Delta p(Q_{\mathrm{sup}})}{\eta_{\mathrm{fan}}} + P_{\mathrm{aux}} \tag{4}$$

The heating and cooling coefficients of performance are $\mathrm{COP_h}$ and $\mathrm{COP_c}$, respectively. The nonnegative latent-cooling load $\dot{Q}_{\mathrm{lat}}$ represents moisture removal at the cooling coil and is consistent with the coil dehumidification rate in the moisture balance. Condensation on interior surfaces is treated separately.

The fan contribution is calculated from total supply flow, system pressure rise Δp, and overall fan–motor efficiency η_{fan}. A measured or prescribed fan-power value may replace this term. Filter pressure losses are included in the system pressure rise, and P_{aux} accounts only for electrical loads excluded from the preceding terms. The contributions included in each numerical scenario are specified with its operating settings.

With state, control, and disturbance vectors defined as:

$$\mathbf{x} = \begin{bmatrix} T & w & c & p_{\mathrm{m}} \end{bmatrix}^{\mathrm{T}},$$
$$\mathbf{u} = \begin{bmatrix} Q_{\mathrm{sup}} & r & \dot{Q}_{\mathrm{HVAC},s} & \dot{m}_{\mathrm{v,HVAC}} \end{bmatrix}^{\mathrm{T}},$$
$$\mathbf{d} = \begin{bmatrix} T_{\mathrm{o}} & w_{\mathrm{o}} & c_{\mathrm{o}} & p_{\mathrm{m,o}} & I_{\mathrm{sol}} & n \end{bmatrix}^{\mathrm{T}}$$

the coupled model is written as:

$$\dot{\mathbf{x}} = f(\mathbf{x}, \mathbf{u}, \mathbf{d}; \boldsymbol{\theta}), \mathbf{y} = \begin{bmatrix} T & w & c & p_{\mathrm{m}} & P_{\mathrm{HVAC}} \end{bmatrix}^{\mathrm{T}} \tag{5}$$

The parameter vector $\boldsymbol{\theta}$ contains the effective thermal properties, infiltration characteristics, solar-gain parameters, occupant source coefficients, filtration and deposition coefficients, and equipment-performance parameters. These quantities are distinguished from the operating inputs and environmental disturbances. The formulation therefore evaluates cabin conditions and electrical demand under the same prescribed ventilation policy, with each response linked to the corresponding heat and mass exchanges.

3 Numerical Implementation and Assessment Methods

3.1 Numerical Formulation and Consistency Assessment

The coupled balances in Section 2 define an initial-value problem,

$$\frac{\mathrm{d}\mathbf{x}}{\mathrm{d}t} = f(t, \mathbf{x}, \mathbf{u}, \mathbf{d}; \boldsymbol{\theta}), \mathbf{x}(0) = \mathbf{x}_0 \tag{6}$$

where, $\mathbf{x} = [T, w, c, p_m]^{\mathrm{T}}$, $\mathbf{u}$ contains the HVAC and ventilation inputs, and $\mathbf{d}$ contains the prescribed environmental and occupancy conditions. The parameter vector $\boldsymbol{\theta}$ retains the definitions introduced in Section 2. Separating parameters from operating inputs allows the effects of ventilation policies to be examined without changing the underlying cabin description.

The summer demonstration uses explicit time integration with a fixed step of $\Delta t = 1.2$ s over a 30-min interval. At each step, the active ventilation mode determines the outdoor-air and recirculation flows, filtration terms, and fan power. The state derivatives are evaluated from the coupled balances, and HVAC electrical power is integrated over the operating interval to obtain cumulative electricity use. The reported initial conditions, airflow settings, thermal parameters, and equipment settings are summarized in Section 4.

For the rule-based policy, the ventilation mode is retained between switching events. The controller changes from high recirculation to fresh-air operation when cabin CO_2 exceeds 1,100 ppm and returns to recirculation when it falls below 850 ppm. The two thresholds introduce hysteresis, preventing immediate reversal at a single switching concentration. Switching is evaluated on the integration grid, so the recorded transition time has the temporal resolution of the numerical step. Comparisons between policies use a common output grid and the same environmental forcing.

Numerical verification examines whether the implementation solves the governing equations correctly, whereas physical validation examines agreement with independent measurements [23]. The numerical assessment considered here comprises step-size comparisons, integrated balance residuals, and analytical solutions for constant-input cases. These diagnostics are distinguished from differences in cabin conditions and electricity use between ventilation policies.

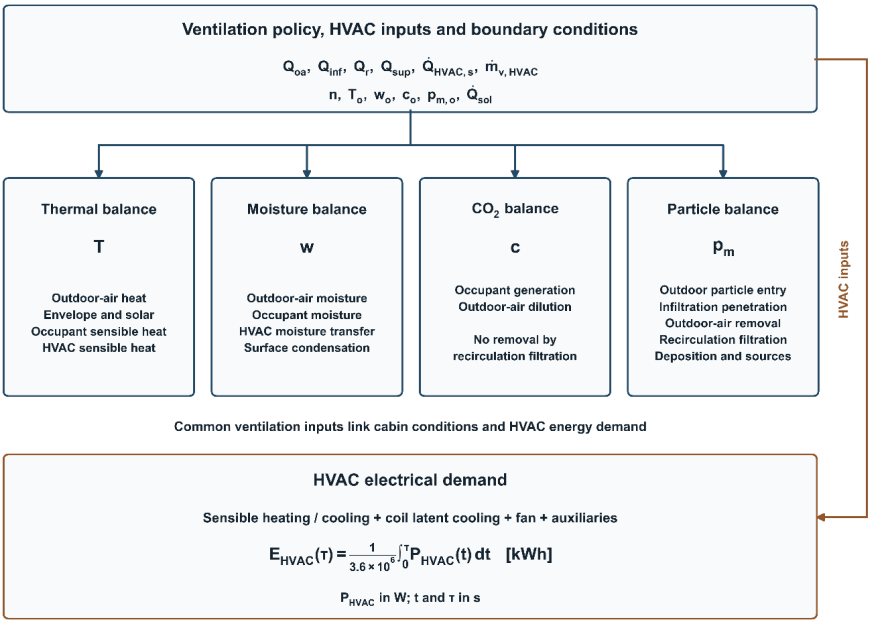


Figure 2. Coupling between cabin heat, moisture, pollutants, and HVAC demand

Note: Q_{oa} = flow rate of controlled outdoor air supplied by the HVAC system; Q_{inf} = uncontrolled outdoor-air exchange; Q_r = flow rate of recirculated cabin air within the HVAC supply; Q_{sup} = supply airflow; $\dot{Q}_{HVAC,s}$ = sensible conditioning rate; $\dot{m}_{v,HVAC}$ = HVAC moisture-transfer rate; n = occupancy; T_o = outdoor temperature; w_o = outdoor humidity ratio; c_o = outdoor CO_2 concentrations; $p_{m,o}$ = outdoor $PM_{2.5}$ concentrations; $\dot{Q}_{sol}$ = solar heat gain rate; T = cabin temperature; w = cabin humidity ratio; c = cabin CO_2 concentrations; P_m = cabin $PM_{2.5}$ concentrations; P_{HVAC} = total electrical power demand of the HVAC system; HVAC = heating, ventilation, and air-conditioning; CO_2 = carbon dioxide; $PM_{2.5}$ = fine particulate matter.

For a state x_i, the normalized difference between solutions obtained with steps h and $h/2$ is defined as:

$$\varepsilon_{i,h} = \frac{\max_{t\in\mathcal{T}} \left| x_i^{(h)}(t) - x_i^{(h/2)}(t) \right|}{\max\left\{ x_{i,\,\text{scale}}\,, \max_{t\in\mathcal{T}} \left| x_i^{(h/2)}(t) \right| \right\}} \tag{7}$$

where, $\mathcal{T}$ is the common comparison grid, and $x_{i,\text{scale}} > 0$ is a characteristic scale with the same units as the state variable. This scale prevents division by a near-zero reference magnitude. Under threshold-based operation, state differences are assessed alongside switching times and cumulative electricity use because small concentration differences near a threshold can change the transition time.

An integrated balance residual provides a complementary check on the numerical solution. For a stored quantity M, the residual is:

$$R_M(t) = M(t) - M(0) - \int_0^t \left[\dot{M}_{\text{in}}(s) - \dot{M}_{\text{out}}(s) + \dot{M}_{\text{source}}(s) \right] \mathrm{d}s$$

The residual measures the difference between the change in storage and the integrated net transfer. All terms must use consistent units, with $\dot{M}_{\text{source}}$ representing net internal production or removal. For the CO_2 balance, the stored quantity is the equivalent CO_2 volume Vc under the adopted reference conditions. For the $PM_{2.5}$ balance, it is the particle mass Vp_m. Residuals are interpreted relative to an explicitly stated storage or transfer scale.

Under constant occupancy, outdoor concentration, and effective outdoor-air exchange, the CO_2 balance has the analytical solution:

$$c(t) = c_o + \frac{G_{CO_2}}{Q_f} + \left[c(0) - c_o - \frac{G_{CO_2}}{Q_f} \right] \exp\left(-\frac{Q_f t}{V} \right), G_{CO_2} = n g_{CO_2} \tag{8}$$

for $Q_f > 0$. The equilibrium concentration is $c_o + G_{CO_2}/Q_f$, and the response time is V/Q_f. These expressions connect the concentration trajectory directly to occupancy and ventilation. When $Q_f = 0$, the corresponding limit is $c(t) = c(0) + G_{CO_2} t/V$.

A similar reference is available for $PM_{2.5}$ under constant conditions. Define:

$$a_{\mathrm{p}} = \frac{Q_{\mathrm{oa}} + Q_{\mathrm{inf}} + \eta_{\mathrm{r}} Q_{\mathrm{r}}}{V} + k_{\mathrm{d}},$$
$$b_{\mathrm{p}} = \frac{\left[(1-\eta_{\mathrm{f}})\, Q_{\mathrm{oa}} + p_{\mathrm{inf}} Q_{\mathrm{inf}}\right] p_{\mathrm{m,o}} + S_{\mathrm{m}}}{V}$$

Eq. (3) then gives:

$$p_{\mathrm{m}}(t) = p_{\mathrm{m},\infty} + \left[p_{\mathrm{m}}(0) - p_{\mathrm{m},\infty}\right] e^{-a_{\mathrm{p}} t}, p_{\mathrm{m},\infty} = \frac{b_{\mathrm{p}}}{a_{\mathrm{p}}} \tag{9}$$

for $a_{\mathrm{p}} > 0$. Here, a_{p} is the total first-order removal coefficient and b_{p} is the concentration source rate. This form distinguishes particle entry from removal by outdoor-air exchange, recirculation filtration, and deposition. Eqs. (8) and (9) provide exact reference trajectories when the corresponding source terms, boundary conditions, airflow rates, and removal coefficients remain constant. For piecewise-constant operation, each segment uses the terminal concentration of the preceding segment as its initial condition.

3.2 Performance Comparison and Parameter Sensitivity

The policy comparison reports cabin temperature, relative humidity, CO_2 concentration, $PM_{2.5}$ concentration, and cumulative HVAC electricity use over the same operating interval. Temperature and relative humidity characterize the mean thermal and moisture response, while pollutant concentrations describe CO_2 accumulation and particle loading. Reporting these trajectories alongside electricity use reveals the environmental conditions associated with each policy's energy demand.

For a trajectory y_i and a corresponding reference y_i^{ref}, their difference at sampling instant i is:

$$e_i = y_i - y_i^{\mathrm{ref}} \tag{10}$$

The reference may be an analytical solution for numerical assessment or another ventilation policy for an operating comparison. Its origin determines the meaning of the difference. Mean absolute difference, MAD; root-mean-square difference, RMSD; and mean signed difference, $\bar{e}$ are defined as:

$$\mathrm{MAD} = \frac{1}{N}\sum_{i=1}^{N} |e_i|$$
$$\mathrm{RMSD} = \sqrt{\frac{1}{N}\sum_{i=1}^{N} e_i^2}$$
$$\bar{e} = \frac{1}{N}\sum_{i=1}^{N} e_i$$

where, N is the number of paired samples. Comparison with an analytical solution quantifies numerical discrepancy, whereas comparison between ventilation policies quantifies differences in their predicted responses. The perturbed points in figures are illustrative and are excluded from accuracy assessment.

For cumulative HVAC electricity use, the relative difference between a policy a and a reference policy is:

$$\delta_E^{a|\,\mathrm{ref}} = \frac{E_{\mathrm{HVAC},\,a} - E_{\mathrm{HVAC,ref}}}{E_{\mathrm{HVAC,ref}}} \times 100\%, E_{\mathrm{HVAC,ref}} > 0 \tag{11}$$

A negative value indicates lower electricity use than the reference policy. All policies are evaluated over the same duration and use the same definitions of included electrical loads. Airflow rates and fan-power settings may differ as prescribed by each policy. The resulting energy difference therefore characterizes the complete operating configuration. Final concentrations and transient responses are reported alongside energy use.

Parameter sensitivity examines how the calculated outcomes depend on the assumptions entering the model. For a selected scalar output Y,

$$Y = \mathcal{M}\left(\boldsymbol{\theta}, \mathbf{u}, \mathbf{d}, \mathbf{x}_0; \tau\right) \tag{12}$$

where, $\mathcal{M}$ denotes the simulation and output calculation over duration τ. Relevant outputs include final or peak pollutant concentrations, cabin temperature, and cumulative HVAC electricity use. The sensitivity illustration in Section 4 focuses on electricity use at the end of the 30-min summer case.

For a positive continuous parameter θ_j and nonzero baseline output Y_0, the normalized local sensitivity is:

$$S_j = \frac{\theta_{j,0}}{Y_0}\frac{\partial Y}{\partial \theta_j}\bigg|_{\boldsymbol{\theta}=\boldsymbol{\theta}_0} \approx \frac{Y\left(\boldsymbol{\theta}_0 + \Delta\theta_j \mathbf{e}_j\right) - Y\left(\boldsymbol{\theta}_0 - \Delta\theta_j \mathbf{e}_j\right)}{2\delta Y_0}, \Delta\theta_j = \delta\theta_{j,0} \tag{13}$$

where, $\mathbf{e}_j$ is the unit vector selecting parameter j, and $\delta = 0.10$ specifies the nominal ±10% perturbation for continuous parameters. Each parameter is varied separately while all other inputs retain their baseline values. Both perturbed values must remain within the parameter's admissible range. Positive sensitivity indicates that increasing the parameter raises the selected output; negative sensitivity indicates the opposite. The coefficient describes the local response around the stated operating point.

Occupant count is treated as a discrete input. Comparisons between integer occupant counts change sensible heat release, moisture production, and CO_2 generation consistently. A fractional perturbation of a per-person source rate instead represents variation in occupant activity or source strength and is identified by the specific parameter being varied.

Trajectory comparisons quantify the differences between ventilation policies, while local sensitivity coefficients describe their dependence on selected model inputs. The combined assessment links electricity use and cabin conditions to outdoor-air exchange, filtration, deposition, and thermal loads under the prescribed scenario.

4 Simulated Scenarios and Coupled Trade-Offs

4.1 Summer Scenario and Ventilation Policies

Three ventilation policies are compared over a prescribed 30-min summer scenario with four occupants, a warm outdoor environment, and elevated outdoor $PM_{2.5}$. The comparison examines how outdoor-air exchange affects CO_2 dilution, particle ingress, cooling demand, and cumulative HVAC electricity use.

The outdoor temperature is held at 35 ℃, with CO_2 and $PM_{2.5}$ concentrations of 430 ppm and 80 μg/m^3, respectively. The effective cabin volume is 3 m^3. All policies start from a cabin temperature of 35 ℃, CO_2 concentration of 430 ppm, $PM_{2.5}$ concentration of 8.0 μg/m^3, and relative humidity of 35.3%. The effective thermal capacitance is 130 kJ·K^{-1}, the envelope conductance is 40 W·K^{-1}, and the solar heat gain is 450 W. Table 2 summarizes the reported scenario settings.

Table 2. Parameters and operating settings for the summer simulation

Quantity	Value or Specification
Simulation duration	30 min
Integration step	1.2 s
Cabin volume, V	3 m^3
Occupancy, n	Four occupants
Outdoor temperature, T_o	35 ℃
Outdoor CO_2 concentration	430 ppm
Outdoor $PM_{2.5}$ concentration	80 μg/m^3
Initial cabin temperature	35 ℃
Initial cabin CO_2 concentration	430 ppm
Initial cabin $PM_{2.5}$ concentration	8.0 μg/m^3
Initial cabin relative humidity	35.3%
Effective thermal capacitance, C_{th}	130 kJ·K^{-1}
Envelope conductance, UA	40 W·K^{-1}
Solar heat gain, $\dot{Q}_{sol}$	450 W
Effective outdoor-air exchange in fresh-air mode	120 m^3·h^{-1}
Effective outdoor-air exchange in recirculation mode	8 m^3·h^{-1}, attributed to leakage
Filtered recirculation flow	45 m^3·h^{-1}
Prescribed PM inlet penetration coefficient	0.45
Recirculation filter efficiency	0.70
Particle deposition rate	1.2 h^{-1}
Maximum sensible cooling rate	2,500 W
Cooling coefficient of performance	2.8
Fan electrical power	Fresh air: 95 W; recirculation: 65 W
CO_2 switching thresholds	Fresh air above 1,100 ppm; recirculation below 850 ppm

Note: CO_2 = carbon dioxide; $PM_{2.5}$ = fine particulate matter; PM = particulate matter.

Continuous fresh-air operation, denoted F, maintains a prescribed effective outdoor-air exchange of 120 $m^3 \cdot h^{-1}$. High-recirculation operation, denoted R, combines a filtered recirculation flow of 45 $m^3 \cdot h^{-1}$ with an effective outdoor-air exchange of 8 $m^3 \cdot h^{-1}$ attributed to leakage. Fan electrical power is 95 W in mode F and 65 W in mode R. The comparison therefore evaluates complete operating configurations with different airflow and fan-power settings.

The rule-based policy, denoted B, starts in mode R and switches to mode F when cabin CO_2 exceeds 1,100 ppm. It returns to mode R when CO_2 falls below 850 ppm and retains the current mode between these thresholds. The thresholds define the hysteresis rule adopted for this scenario.

Sensible cooling is prescribed by:

$$\dot{Q}_{\text{cool}}(t) = \min\left\{\dot{Q}_{\max}, K_T \max\left[T_{\circ\text{C}}(t) - T_{\text{set}}, 0\right]\right\}$$

The cooling-capacity limit is $\dot{Q}_{\max} = 2500$ W, the proportional gain is $K_T = 500$ W·K^{-1}, and the temperature reference is $T_{\text{set}} = 24$ °C. Here, $T_{\circ\text{C}}$ is cabin temperature expressed in degrees Celsius, with $T_{\circ\text{C}} = T - 273.15$ when the temperature state is expressed in kelvin. The sensible-conditioning input in Eq. (1) is $\dot{Q}_{\text{HVAC,s}} = -\dot{Q}_{\text{cool}}$. The sensible-cooling electrical contribution is $\dot{Q}_{\text{cool}}/2.8$, and the prescribed fan power replaces the pressure–flow term in Eq. (4). The 24 °C reference determines the proportional cooling response; continuing thermal loads can produce an equilibrium cabin temperature above this value.

Cabin conditions are compared through their transient trajectories and the values reported at five-minute intervals. For a concentration $C(t)$, the time average over the operating duration τ is defined as:

$$\bar{C} = \frac{1}{\tau}\int_0^{\tau} C(t)\mathrm{d}t \tag{14}$$

The time average incorporates the concentration trajectory over the full interval and differs from the final concentration. It characterizes the mean cabin concentration rather than an inhaled dose.

With power expressed in watts and time in seconds, cumulative HVAC electricity use is:

$$E_{\text{HVAC}}(\tau) = \frac{1}{3.6 \times 10^6}\int_0^{\tau} P_{\text{HVAC}}(t)\mathrm{d}t \text{ kWh} \tag{15}$$

Applying Eq. (11) with continuous fresh-air operation as the reference gives:

$$\Delta E^{a|\text{F}} = \frac{E_{\text{HVAC},a} - E_{\text{HVAC, F}}}{E_{\text{HVAC, F}}} \times 100\% \tag{16}$$

Negative values indicate lower electricity use. This comparison is interpreted alongside pollutant concentrations and thermal conditions, since the ventilation policies do not produce equivalent cabin environments.

4.2 Cabin Response and Energy–Air-Quality Trade-Offs

Figure 3 shows the simulated cabin-temperature response together with reference points generated by perturbing model output. These points provide a graphical illustration of the trajectory and are not independent measurements. The temperature response is reported alongside pollutant concentrations, relative humidity, and cumulative electricity use in Table 3, allowing the consequences of each ventilation policy to be compared over the same interval.

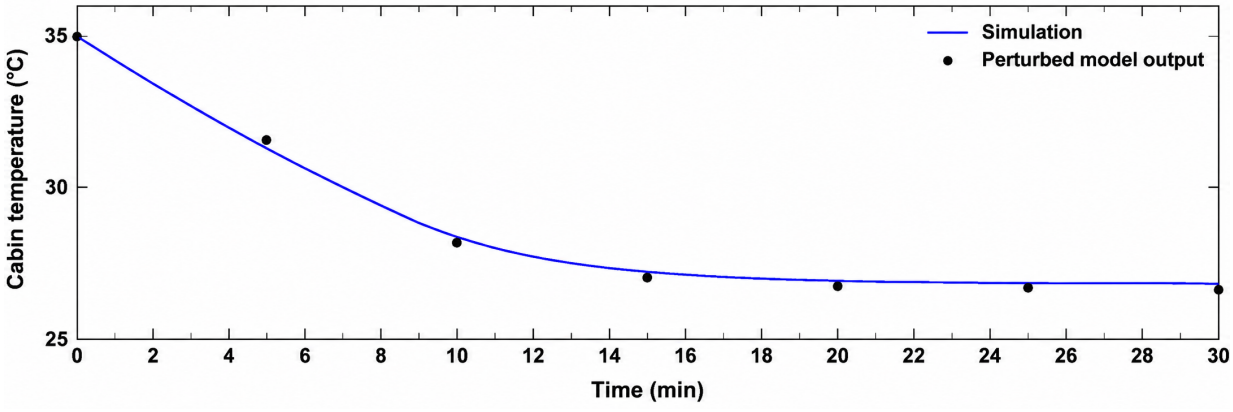


Figure 3. Simulated cabin temperature and perturbed model output

Table 3. Simulated summer cabin conditions and cumulative HVAC electricity use

Mode	Time (min)	Temperature (°C)	CO_2 (ppm)	$PM_{2.5}$ (μg/m^3)	Relative Humidity (%)	Electricity Use (kWh)
Fresh air	0	35.0	430	8.0	35.3	0.000
Fresh air	5	31.3	1,009	34.1	43.5	0.082
Fresh air	10	28.3	1,029	34.9	51.7	0.163
Fresh air	15	27.2	1,030	35.0	55.2	0.226
Fresh air	20	26.9	1,030	35.0	56.2	0.279
Fresh air	25	26.8	1,030	35.0	56.5	0.329
Fresh air	30	26.8	1,030	35.0	56.5	0.379
Recirculation	0	35.0	430	8.0	35.3	0.000
Recirculation	5	31.2	2,224	7.1	44.0	0.080
Recirculation	10	27.9	3,661	6.8	53.2	0.156
Recirculation	15	26.7	4,811	6.7	57.2	0.209
Recirculation	20	26.4	5,731	6.7	58.6	0.252
Recirculation	25	26.3	6,469	6.7	59.2	0.292
Recirculation	30	26.3	7,059	6.7	59.4	0.332
Rule-based	0	35.0	430	8.0	35.3	0.000
Rule-based	5	31.3	1,038	32.1	43.5	0.081
Rule-based	10	28.3	1,030	34.9	51.7	0.162
Rule-based	15	27.2	1,030	34.9	55.2	0.225
Rule-based	20	26.9	1,030	35.0	56.2	0.278
Rule-based	25	26.8	1,030	35.0	56.5	0.328
Rule-based	30	26.8	1,030	35.0	56.5	0.378

Note: HVAC = heating, ventilation, and air-conditioning; CO_2 = carbon dioxide; $PM_{2.5}$ = fine particulate matter.

Cabin temperature decreased from 35.0 ℃ under all three policies. After five minutes, the fresh-air and recirculation configurations reached 31.3 and 31.2 ℃, respectively. Their final temperatures were 26.8 and 26.3 ℃. Both remained above the 24 ℃ reference of the proportional cooling law because a positive temperature difference was required to sustain cooling against the continuing thermal loads.

The CO_2 responses differed substantially. Under fresh-air operation, the concentration reached 1,009 ppm after five minutes and approached approximately 1,030 ppm thereafter. Under high recirculation, it increased to 2,224 ppm after five minutes and 7,059 ppm after 30 min. The lower outdoor-air exchange in mode R restricted dilution of the occupant-generated source, producing continued accumulation over the simulated interval.

$PM_{2.5}$ followed the opposite pattern. Fresh-air operation increased cabin concentration from 8.0 to 34.1 μg/m^3 within five minutes and to approximately 35.0 μg/m^3 at 30 min. Under recirculation, concentration decreased to approximately 6.7 μg/m^3 as filtration and deposition removed particles while limited outdoor-air exchange restricted their entry. Based on the rounded values in Table 3, the final recirculation concentration was approximately 80.9% lower than the fresh-air value. This percentage compares endpoint concentrations, rather than time-averaged concentrations or inhaled doses.

Figure 4 presents these contrasting pollutant trajectories. Greater outdoor-air exchange diluted internally generated CO_2 but increased particle ingress from the polluted surroundings, consistent with the ventilation-dependent behavior reported in previous vehicle studies [4, 5]. The magnitude of the response here depends on the prescribed airflow, penetration, filtration, and deposition parameters.

Relative humidity increased as the cabin cooled, reaching 56.5% under fresh-air operation and 59.4% under recirculation. Relative humidity depends on both temperature and water-vapour content; its higher value under recirculation alone does not establish a larger increase in humidity ratio.

Cumulative electricity use reached 0.379 kWh under fresh-air operation and 0.332 kWh under recirculation at 30 min. Based on the rounded table values, the difference was 0.047 kWh, equivalent to approximately 12.4% of the fresh-air total. This difference reflects both the lower outdoor-air conditioning load and the lower prescribed fan power in mode R.

Over 30 min, the prescribed fan powers contributed 0.0475 kWh in mode F and 0.0325 kWh in mode R. Their difference of 0.015 kWh accounted for approximately 32% of the reported total energy gap. The remaining difference arose from the conditioning contribution included in the energy calculation. The comparison therefore concerns the complete operating configurations, rather than recirculation fraction alone. Figure 5 presents the temperature and cumulative electricity-use trajectories.

Policy B approached the response of continuous fresh-air operation after the initial switching period. CO_2 was

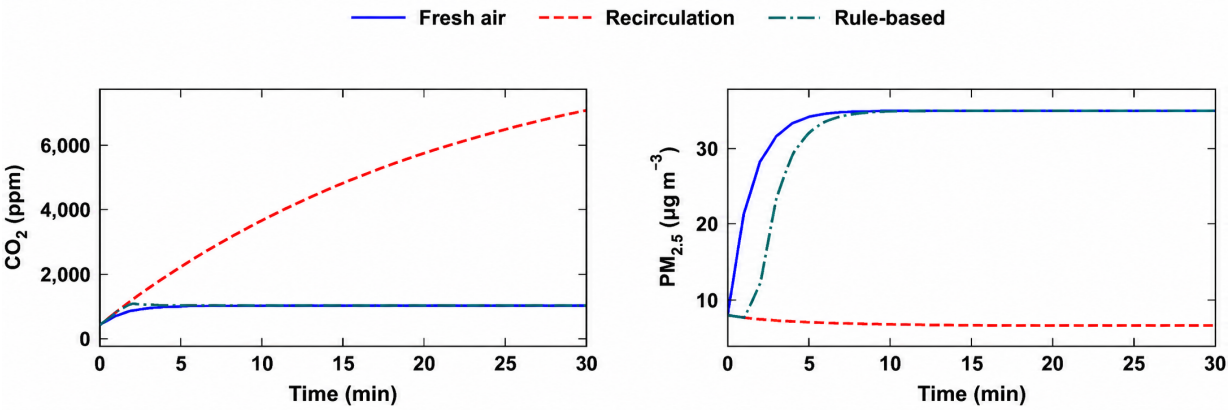


Figure 4. Simulated CO_2 and $PM_{2.5}$ trajectories under three ventilation policies

Note: CO_2 = carbon dioxide; $PM_{2.5}$ = fine particulate matter.

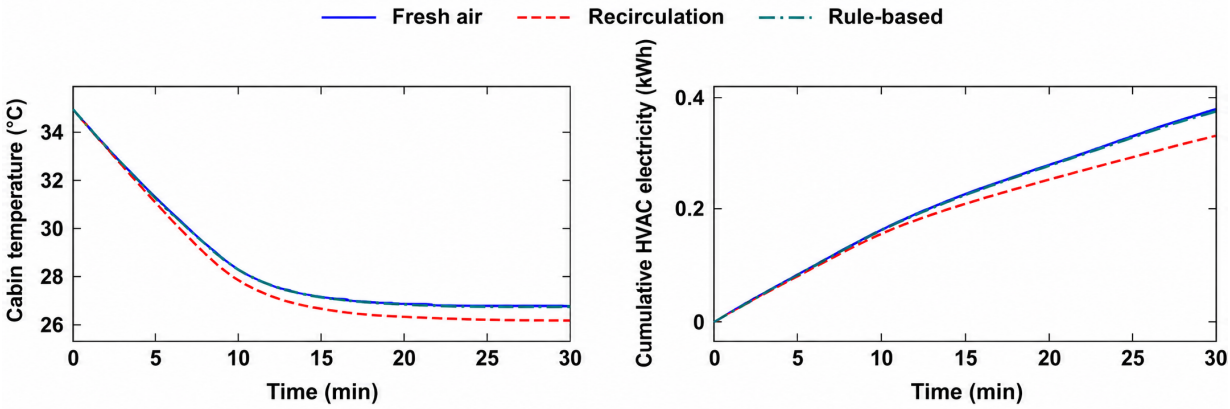


Figure 5. Cabin temperature and cumulative HVAC electricity use under three ventilation policies

Note: HVAC = heating, ventilation, and air-conditioning.

1,038 ppm after five minutes and approximately 1,030 ppm at 30 min. Final temperature, $PM_{2.5}$ concentration, and relative humidity matched mode F at the precision reported in Table 3. Electricity use was 0.378 kWh, approximately 0.3% below mode F based on the rounded totals.

This behavior followed from the position of the switching thresholds relative to the fresh-air CO_2 equilibrium. After switching to mode F, the concentration approached approximately 1,030 ppm, above the 850 ppm threshold required to restore recirculation. The controller consequently retained fresh-air operation. The selected rule prevented the continued CO_2 accumulation observed in mode R, while its return threshold limited subsequent use of recirculation.

Figure 6 presents the local sensitivity illustration for HVAC electricity use at 30 min around the fresh-air baseline. Eq. (13) defines the normalized response to individual continuous-parameter perturbations. Unlike the ventilation-policy comparison, which changes several operating settings together, this analysis examines the response to individual input changes around a common baseline.

5 Discussion and Engineering Implications

5.1 Interpreting Energy Savings Alongside Cabin Conditions

The summer comparison demonstrates that the energy performance of a ventilation configuration must be interpreted alongside the cabin conditions it produces. Recirculation reduced electricity use and particle concentration but restricted the removal of occupant-generated CO_2. Fresh-air operation produced the opposite balance. The engineering question is therefore which configuration satisfies the required environmental conditions at an acceptable electrical demand.

The reported 12.4% energy difference includes changes in both outdoor-air exchange and fan power. The prescribed fan-power difference contributed 0.015 kWh over 30 min, accounting for approximately 32% of the total gap. This decomposition shows why conditioning and air-circulation power should be reported separately, consistent with research examining the contribution of blower operation to vehicle HVAC energy consumption [22].

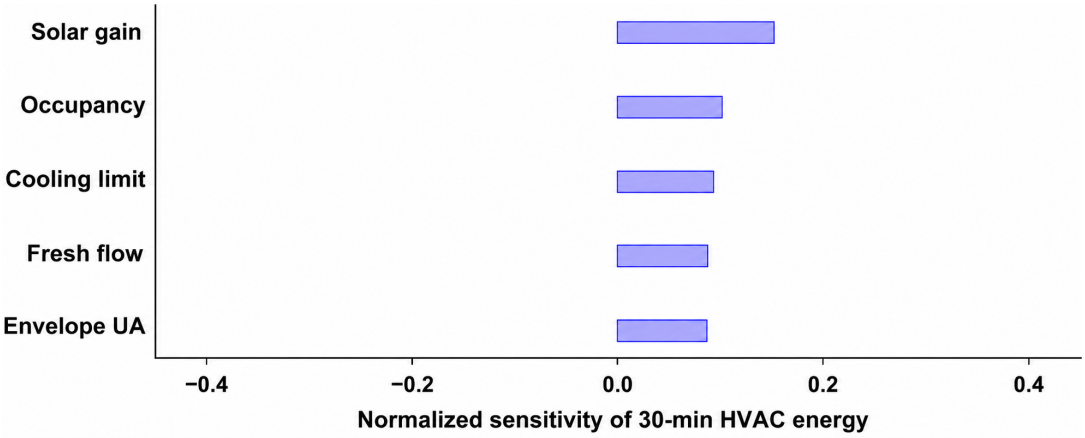


Figure 6. Local sensitivity of 30-min HVAC electricity use around the fresh-air baseline
Note: HVAC = heating, ventilation, and air-conditioning; UA = envelope conductance.

The configurations also ended at different temperatures and pollutant concentrations. Their energy difference consequently describes the response to two sets of operating inputs, rather than the energy required to maintain equivalent cabin conditions. A comparison at equivalent environmental performance would require common thermal and air-quality targets, with each configuration adjusted to meet them. Reporting the state trajectories together with electricity use makes this distinction explicit.

The direction of the response is consistent with previous studies linking recirculation to changes in particle concentration, CO_2 accumulation, and conditioning demand [4–7]. The contribution here is the separation of these effects into identifiable airflow, filtration, thermal-load, and electrical-demand terms. This structure explains the calculated energy difference without assigning it entirely to recirculation fraction.

5.2 Ventilation Constraints and Threshold-Based Operation

The opposing pollutant responses arise from different source and removal mechanisms. CO_2 is generated inside the cabin and removed through outdoor-air exchange. Recirculation filtration provides no corresponding CO_2 removal mechanism. For particles, recirculation provides repeated filtration while reducing the intake of polluted outdoor air. These mechanisms explain why a policy selected solely to reduce $PM_{2.5}$ can permit substantial CO_2 accumulation, as also observed in experimental vehicle-cabin research [5].

The rule-based result illustrates how switching thresholds interact with ventilation capacity. Once policy B entered fresh-air mode, CO_2 approached an equilibrium above the threshold required to restore recirculation. Fresh-air operation therefore persisted, and the thermal, particle, and energy responses approached those of policy F.

From Eq. (8), the fresh-air equilibrium under constant occupancy and boundary conditions is:

$$c_{\infty,\mathrm{F}} = c_{\mathrm{o}} + \frac{n g_{\mathrm{CO_2}}}{Q_{\mathrm{f,\ F}}}.$$

When the concentration at entry to fresh-air mode exceeds this equilibrium, it approaches the equilibrium from above. A return threshold below that value cannot be reached through continued fresh-air operation under the same conditions. In this comparison, the equilibrium concentration and switching thresholds are expressed in ppm.

For the selected threshold pair, the controller retained fresh-air operation after the initial transition. This result connects threshold selection directly to occupant generation, outdoor CO_2 concentration, and available outdoor-air exchange. Related studies have incorporated CO_2-responsive ventilation and humidity-dependent recirculation into vehicle HVAC control [19, 20]. The present balance model provides a compact explanation of the equilibrium condition governing the switching response.

5.3 Physical Interpretation and Model Applicability

The four-state formulation connects outdoor-air exchange with cabin heat, moisture, and CO_2 transport, while the particle balance additionally represents penetration, filtration, and deposition. The electrical-demand calculation then relates conditioning and air circulation to energy use. Keeping these contributions separate allows an operating change to be followed through the model without counting the same physical exchange twice.

The single-zone representation assumes that cabin mixing occurs sufficiently rapidly relative to the environmental

response being examined. A timescale ratio provides a useful criterion:

$$\varepsilon_{\mathrm{m}} = \frac{\tau_{\mathrm{mix}}}{\tau_{\mathrm{env}}} \tag{17}$$

where, τ_{mix} is the characteristic mixing time and τ_{env} is the shortest environmental response time relevant to the analysis. A small ratio is consistent with representing the cabin through well-mixed states. Here, the ratio defines an applicability criterion rather than a measured characteristic of the simulated cabin.

Mean cabin conditions and local occupant conditions require different spatial descriptions. Supply jets, asymmetric radiation, surface temperatures, and breathing-zone gradients can produce local conditions that differ from the cabin mean. Two-zone thermal models [9] and coupled computational fluid dynamics–thermoregulation models [19] provide additional spatial information. Thermal-comfort models and equivalent-temperature methods also incorporate quantities beyond mean air temperature [10–12]. The present temperature and humidity states characterize bulk cabin conditions and conditioning loads.

Humidity interpretation requires similar care. Relative humidity changes with both temperature and water-vapour content, so its increase during cooling does not by itself quantify moisture accumulation. Windscreen condensation further depends on the interior glass temperature relative to the cabin-air dew point. A mean-air calculation therefore requires a glass-temperature input or an additional thermal submodel to assess condensation potential.

Numerical verification and physical validation provide different forms of evidence [23]. Analytical solutions, step-size comparisons, and conservation residuals provide numerical verification diagnostics, whereas independent measurements provide evidence for physical validation [23]. Independent measurements assess agreement with a physical cabin. The perturbed model outputs in Figure 3 serve as a graphical illustration and provide neither an independent numerical check nor experimental validation. The values reported in Section 4 are model outputs for the prescribed scenario.

5.4 Implications for Energy-Efficient Heating, Ventilation, and Air-Conditioning Assessment

The framework supports HVAC assessment by connecting electricity use with the environmental consequences of each ventilation policy. Separating conditioning and fan power identifies the sources of an energy difference, while the concentration trajectories show how that difference accompanies changes in CO_2 dilution and particle removal. The switching analysis further explains how controller settings determine the time spent in each operating mode.

Applying the formulation to a specific vehicle requires a consistent set of cabin, airflow, filtration, and equipment parameters. Cabin volume, effective thermal capacitance, envelope conductance, leakage, filter performance, and HVAC efficiency define the physical system. Outdoor conditions and occupancy define the operating case. Keeping these quantities distinct from the conservation equations allows ventilation policies to be compared using the same underlying vehicle description.

The relevance to sustainable vehicle energy use lies in coordinating conditioning demand with cabin environmental requirements. Reduced outdoor-air intake can lower electrical demand while increasing CO_2 accumulation; greater outdoor-air exchange can improve dilution while increasing cooling loads and particle entry under polluted conditions. Evaluating these effects together provides a basis for identifying energy-efficient operating choices within specified thermal and air-quality constraints.

6 Conclusions

A reduced-order dynamic model was developed to couple passenger-car cabin temperature, humidity ratio, CO_2 concentration, and $PM_{2.5}$ concentration with HVAC electrical demand. The formulation distinguishes controlled outdoor-air supply, infiltration, and recirculation filtration within a common set of conservation balances. This separation provides a traceable basis for comparing ventilation configurations and explaining their thermal, air-quality, and energy consequences.

In the prescribed 30-min summer scenario with four occupants, high recirculation consumed 0.332 kWh, compared with 0.379 kWh under continuous fresh-air operation. The difference was approximately 12.4%, based on the rounded results. At 30 min, $PM_{2.5}$ concentrations were 6.7 $\mu g/m^3$ under recirculation and 35.0 $\mu g/m^3$ under fresh air, whereas CO_2 concentrations were approximately 7,059 and 1,030 ppm, respectively. Final cabin temperatures were 26.3 and 26.8 °C. The lower electricity use therefore accompanied different cabin conditions. The prescribed fan-power difference accounted for approximately 32% of the total energy gap, demonstrating the importance of separating air-circulation power from conditioning demand.

The CO_2-based switching policy consumed 0.378 kWh and approached the thermal and pollutant outcomes of continuous fresh-air operation. After the initial transition, the fresh-air CO_2 equilibrium remained above the return threshold, so the controller retained fresh-air operation. This result identifies the relationship between threshold selection, occupant generation, outdoor concentration, and available ventilation capacity.

The framework connects vehicle HVAC energy efficiency with the cabin conditions produced by each operating policy. Its contribution is the consistent accounting of airflow pathways, pollutant removal, conditioning loads, and electrical demand within a compact dynamic formulation. For the stated scenario, the comparison shows how energy reductions redistribute thermal and pollutant loads, providing a basis for assessing ventilation choices against defined cabin environmental requirements.

Author Contributions

Conceptualization, A.C. and A.M.; methodology, A.C.; software, A.M.; validation, A.C., A.M., and R.R.; formal analysis, A.M.; investigation, A.M. and R.R.; resources, A.C.; data curation, R.R.; writing—original draft preparation, A.M.; writing—review and editing, A.C., A.M., and R.R.; visualization, R.R.; supervision, A.C.; project administration, A.C.; funding acquisition, A.C. All authors have read and agreed to the published version of the manuscript.

Data Availability

The data used to support the research findings are available from the corresponding author upon request.

Conflicts of Interest

The authors declare no conflicts of interest.

References

[1] G. Lee, J. Song, Y. Lim, and S. Park, "Energy consumption evaluation of passenger electric vehicle based on ambient temperature under real-world driving conditions," *Energy Convers. Manage.*, vol. 306, p. 118289, 2024. https://doi.org/10.1016/j.enconman.2024.118289

[2] Z. Zhu, Y. Zhang, A. Chen, J. Chen, Y. Wu, X. Wang, and T. Fei, "Review of integrated thermal management system research for battery electrical vehicles," *J. Energy Storage*, vol. 106, p. 114662, 2025. https://doi.org/10.1016/j.est.2024.114662

[3] R. C. Geleta, M. F. B. Suhaimi, D. S. Jang, J. K. Kim, D. Lee, and H. Lee, "Advanced control strategies for energy-efficient electric vehicle cabin air conditioning systems: A review," *Energies*, vol. 19, no. 13, p. 3053, 2026. https://doi.org/10.3390/en19133053

[4] D. Wei, F. Nielsen, H. Karlsson, L. Ekberg, and J.-O. Dalenbäck, "Vehicle cabin air quality: Influence of air recirculation on energy use, particles, and CO_2," *Environ. Sci. Pollut. Res.*, vol. 30, no. 15, pp. 43 387–43 402, 2023. https://doi.org/10.1007/s11356-023-25219-x

[5] P. Mohan and G. K. Varghese, "Simultaneous control of carbon dioxide and particulate matter inside a car cabin," *Transp. Res. Part D Transp. Environ.*, vol. 133, p. 104301, 2024. https://doi.org/10.1016/j.trd.2024.104301

[6] L. Russi, P. Guidorzi, B. Pulvirenti, D. Aguiari, G. Pau, and G. Semprini, "Air quality and comfort characterisation within an electric vehicle cabin in heating and cooling operations," *Sensors*, vol. 22, no. 2, p. 543, 2022. https://doi.org/10.3390/s22020543

[7] M. Lesage, D. Chalet, J. Migaud, and C. Krautner, "Optimization of air quality and energy consumption in the cabin of electric vehicles using system simulation," *J. Environ. Manage.*, vol. 358, p. 120861, 2024. https://doi.org/10.1016/j.jenvman.2024.120861

[8] L. Zhao, Q. Zhou, and Z. Wang, "A systematic review on modelling the thermal environment of vehicle cabins," *Appl. Therm. Eng.*, vol. 257, p. 124142, 2024. https://doi.org/10.1016/j.applthermaleng.2024.124142

[9] B. Torregrosa-Jaime, F. Bjurling, J. M. Corberán, F. Di Sciullo, and J. Payá, "Transient thermal model of a vehicle's cabin validated under variable ambient conditions," *Appl. Therm. Eng.*, vol. 75, pp. 45–53, 2015. https://doi.org/10.1016/j.applthermaleng.2014.05.074

[10] B. Chen, Y. Lian, L. Xu, Z. Deng, F. Zhao, H. Zhang, and S. Liu, "State-of-the-art thermal comfort models for car cabin environment," *Build. Environ.*, vol. 262, p. 111825, 2024. https://doi.org/10.1016/j.buildenv.2024.111825

[11] B. Chen, F. Zhao, H. Zhang, Y. Chen, Q. Liu, Z. Deng, and S. Liu, "A multi-dimensional evaluation of existing thermal comfort models for vehicle cabins," *Build. Simul.*, vol. 19, no. 8, pp. 1935–1959, 2026. https://doi.org/10.1007/s12273-026-1439-7

[12] International Organization for Standardization, "Ergonomics of the thermal environment—Evaluation of thermal environments in vehicles—Part 2: Determination of equivalent temperature," ISO 14505-2:2026, 2026. https://www.iso.org/standard/86859.html

[13] D. Wei, F. Nielsen, L. Ekberg, and J.-O. Dalenbäck, "Size-resolved simulation of particulate matters and CO_2 concentration in passenger vehicle cabins," *Environ. Sci. Pollut. Res.*, vol. 29, no. 30, pp. 45 364–45 379, 2022. https://doi.org/10.1007/s11356-022-19078-1

[14] T.-B. Chang, Y.-T. Hsu, and J.-W. Huang, "Optimal ventilation strategies for balancing carbon dioxide and suspended particulate matter concentrations in vehicle cabins," *Atmos. Environ.*, vol. 334, p. 120697, 2024. https://doi.org/10.1016/j.atmosenv.2024.120697

[15] C. Wang, J. Liu, M. He, J. Xu, and H. Liao, "Investigating the filtration performance and service life of vehicle cabin air filters in China," *Environ. Int.*, vol. 190, p. 108939, 2024. https://doi.org/10.1016/j.envint.2024.108939

[16] E. Renck and H. Jung, "The effect of portable air purifiers and cabin air filters on particulate matter and nitrogen oxides concentrations in vehicle cabins," *Environ. Sci.: Processes Impacts*, vol. 27, no. 9, pp. 3029–3037, 2025. https://doi.org/10.1039/D5EM00194C

[17] G. Silva, J. Duarte, J. S. Baptista, and J. C. Rufo, "Low-cost sensors for indoor air quality monitoring: A systematic review of accuracy, applications, and limitations," *J. Air Waste Manage. Assoc.*, vol. 76, no. 5, pp. 315–341, 2026. https://doi.org/10.1080/10962247.2026.2624795

[18] A. K. Persily, "Quit blaming ASHRAE Standard 62.1 for 1000 ppm CO_2," in *The 16th Conference of the International Society of Indoor Air Quality & Climate (Indoor Air 2020)*, Seoul, Republic of Korea, 2020. https://www.nist.gov/publications/quit-blaming-ashrae-standard-621-1000-ppm-co2

[19] A. Ramesh Babu, S. Sebben, Z. Chronéer, and S. Etemad, "An adaptive cabin air recirculation strategy for an electric truck using a coupled CFD-thermoregulation approach," *Int. J. Heat Mass Transfer*, vol. 221, p. 125056, 2024. https://doi.org/10.1016/j.ijheatmasstransfer.2023.125056

[20] M. Lesage, D. Chalet, and J. Migaud, "Optimising ventilation strategies for improved driving range and comfort in electric vehicles," *World Electr. Veh. J.*, vol. 16, no. 2, p. 98, 2025. https://doi.org/10.3390/wevj16020098

[21] W. Wang, J. Ren, X. Yin, Y. Qiao, and F. Cao, "Energy-efficient operation of the thermal management system in electric vehicles via integrated model predictive control," *J. Power Sources*, vol. 603, p. 234415, 2024. https://doi.org/10.1016/j.jpowsour.2024.234415

[22] D. Zhang, J. Ni, and X. Shi, "Study of low-temperature energy consumption optimization of battery electric vehicle air conditioning systems considering blower efficiency," *Processes*, vol. 12, no. 7, p. 1495, 2024. https://doi.org/10.3390/pr12071495

[23] W. L. Oberkampf and C. J. Roy, *Verification and Validation in Scientific Computing*. Cambridge, UK: Cambridge University Press, 2010. https://doi.org/10.1017/CBO9780511760396

[24] E. Hairer and G. Wanner, *Solving Ordinary Differential Equations II: Stiff and Differential-Algebraic Problems*. Berlin, Germany: Springer, 1996. https://doi.org/10.1007/978-3-642-05221-7

[25] SciPy Community, "Integration and ODEs (scipy.integrate)," 2026. https://docs.scipy.org/doc/scipy/reference/integrate.html

[26] Joint Committee for Guides in Metrology, "Evaluation of measurement data—Guide to the expression of uncertainty in measurement," JCGM 100:2008, 2008. https://doi.org/10.59161/JCGM100-2008E

[27] Joint Committee for Guides in Metrology, "Evaluation of measurement data—Supplement 1 to the "Guide to the expression of uncertainty in measurement"— Propagation of distributions using a Monte Carlo method," JCGM 101:2008, 2008. https://doi.org/10.59161/JCGM101-2008

[28] M. D. Morris, "Factorial sampling plans for preliminary computational experiments," *Technometrics*, vol. 33, no. 2, pp. 161–174, 1991. https://doi.org/10.1080/00401706.1991.10484804

[29] A. Saltelli, M. Ratto, T. Andres, F. Campolongo, J. Cariboni, D. Gatelli, M. Saisana, and S. Tarantola, *Global Sensitivity Analysis: The Primer*. Chichester, UK: John Wiley & Sons, 2008. https://doi.org/10.1002/9780470725184